© 2023 Journal of Pharmacy & Pharmacognosy Research, 11 (2), 325-345, 2023
ISSN 0719-4250
https://jppres.com

DOI: https://doi.org/10.56499/jppres23.1606_11.2.325

Original Article

In silico evaluation of the dermal antiaging activity of *Molineria latifolia* (Dryand. ex W.T. Aiton) Herb. Ex Kurz compounds

[Evaluación *in silico* de la actividad antienvejecimiento dérmica de compuestos de *Molineria latifolia* (Dryand. ex W.T. Aiton) Herb. ex Kurz]

Syamsu Nur[1,2], Muhammad Hanafi[3,4], Heri Setiawan[5], Nursamsiar[2], Berna Elya[1*]

[1]Department of Phytochemistry and Pharmacognosy, Faculty of Pharmacy, Universitas Indonesia, Depok, 16424, Indonesia.
[2]Department of Pharmaceutical Chemistry, Sekolah Tinggi Ilmu Farmasi Makassar, Makassar, 90245, Indonesia.
[3]Research Centre for Pharmaceutical Ingredient and Traditional Medicine, National Research and Innovation Agency (BRIN), Serpong, 15314, Indonesia.
[4]Department of Phytochemistry, Faculty of Pharmacy, Pancasila University, South Jakarta, 12640, Indonesia.
[5]Department of Pharmacology, Faculty of Pharmacy, Universitas Indonesia, Depok, 16424, Indonesia.
*E-mail: berna.elya@farmasi.ui.ac.id

Abstract

Context: Dermal aging is one of the events caused by a decrease in the structure of skin tissues due to various factors. *Molineria latifolia* is one of the plants empirically used in medicine and can be developed to treat dermal aging problems.

Aims: To evaluate *M. latifolia* compounds as dermal antiaging, particularly in inhibiting the upregulation of collagenase, gelatinase, and hyaluronidase using an *in silico*.

Methods: Ligands are 46 compounds from *M. latifolia* plant obtained from previous studies and native ligands and target proteins were generated via PubChem and RSCB protein database. *In silico* analyzes were performed using various parameters, namely drug like-ness, absorption, distribution, toxicity prediction, and molecular docking of compounds to the target proteins 2D1N (MMP-13), 1GKC (MMP-9), and 1FCV (hyaluronidase).

Results: Drug-likeness showed that most compounds were suitable according to Lipinski's rule. Analysis of the absorption and distribution of compounds for each parameter gives a different pharmacokinetic profile according to the compound's physicochemical properties. Quercetin and tricosanoic acid were mutagenic, and the compounds aviprin, azedarachin-C, and ubiquinone were carcinogenic genotoxic, and mutagenic. The results of the docking analysis showed that pomiferin, scandenin, mundulone, and rubratoxin had the most negative binding affinity when interacting with the target proteins 2D1N and 1GKC. Meanwhile, orcinol glucoside, orcinol glucoside B, tetrahydroxyflavanone, and sugiol were predicted to interact with the three (MMP-13, MMP-9, and hyaluronidase) target proteins.

Conclusions: Specific compounds of *M. latifolia* were predicted to be developed as candidates for dermal antiaging, and further studies are required.

Keywords: hyaluronidase; matrix metalloproteinase; molecular docking; *Molineria latifolia*; skin antiaging.

Resumen

Contexto: El envejecimiento dérmico es uno de los eventos causados por una disminución en la estructura de los tejidos de la piel debido a diversos factores. *Molineria latifolia* es una de las plantas utilizadas empíricamente en medicina y puede desarrollarse para tratar problemas de envejecimiento dérmico.

Objetivos: Evaluar los compuestos de *M. latifolia* como antienvejecimiento dérmico, en particular en la inhibición de la regulación al alza de la colagenasa, gelatinasa e hialuronidasa utilizando un método *in silico*.

Métodos: Los ligandos son 46 compuestos de la planta *M. latifolia* obtenidos de estudios previos y los ligandos nativos y las proteínas diana se generaron a través de PubChem y la base de datos de proteínas RSCB. Se llevaron a cabo análisis *in silico* utilizando diversos parámetros, a saber, semejanza a fármaco, absorción, distribución, predicción de toxicidad y acoplamiento molecular de los compuestos a las proteínas diana 2D1N (MMP-13), 1GKC (MMP-9) y 1FCV (hialuronidasa).

Resultados: La similitud con los fármacos mostró que la mayoría de los compuestos eran adecuados según la regla de Lipinski. El análisis de la absorción y distribución de los compuestos para cada parámetro da un perfil farmacocinético diferente según las propiedades fisicoquímicas del compuesto. La quercetina y el ácido tricosanoico fueron mutagénicos, y los compuestos aviprin, azedarachin-C y ubiquinona carcinogénicos genotóxicos y mutagénicos. Los resultados del análisis de acoplamiento mostraron que la pomiferina, la escandenina, la mundulona y la rubratoxina tenían la afinidad de unión más negativa cuando interactuaban con las proteínas diana 2D1N y 1GKC. Mientras tanto, se predijo que el glucósido de orcinol, el glucósido de orcinol B, la tetrahidroxiflavanona y el sugiol interactuaban con las tres proteínas diana (MMP-13, MMP-9 e hialuronidasa).

Conclusiones: Se predijo que compuestos específicos de *M. latifolia* podrían desarrollarse como candidatos para el antienvejecimiento dérmico, y se requieren estudios adicionales.

Palabras Clave: acoplamiento molecular; antienvejecimiento cutáneo; hialuronidasa; matriz metaloproteinasa; *Molineria latifolia*.

ARTICLE INFO
Received: February 11, 2023.
Accepted: April 21, 2023.
Available Online: May 2, 2023.

AUTHOR INFO
ORCID: 0000-0001-7730-4414 (SN)
0000-0003-4127-5281 (MH)
0000-0002-0170-9885 (HS)
0000-0001-5923-8812 (N)
0000-0003-2904-6515 (BE)

INTRODUCTION

Aging is a change due to the loss of the ability of a tissue to repair, replace, and maintain the normal structure and function of cells that occur slowly with age (Pyo et al., 2020). Based on world population data, there has been a significant increase in the proportion of the elderly population (over 65 years), from around 8% in 1950 to around 11% in 2009, and it is expected to reach 20% in 2050 (World Health Organization, 2013). This will cause health problems related to aging, including dermal aging, which will also increase. Dermal aging is seen as a decrease in the biological function of chronological age. Generally, aging is unavoidable and proceeds at different speeds, depending on a person's genetics, environment, and lifestyle so aging can occur earlier or later depending on everyone's health. The aging process is marked by a decrease in cellular energy, which reduces the ability of cells to repair themselves. Two phenomena occur, including physiological decline and an increase in disease (Colloca et al., 2020; Nur et al., 2021).

Molecularly, reactive oxygen species (ROS) are thought to play an important role in dermal extracellular matrix changes during intrinsic and photoaging. ROS triggers downstream signaling pathways, including activation of mitogen-activated protein kinase (MAPK) and nuclear factor-κB (NF-κB), and transcription factor-activating protein-1 (AP-1). Activated NF-κB and AP-1 suppress collagen production and increase MMP gene transcription, decreasing collagen content in photoaged skin (Kim and Park, 2016; Nur et al., 2023). Activation of AP-1 also induces an increase in extracellular matrix proteins, namely matrix metalloproteinases (MMPs), including MMP-1 (collagenase) and MMP-9 (gelatinase), and hyaluronidase. The increased production of matrix tissue degrading enzymes in the skin causes premature aging, characterized by the formation of wrinkles and sagging (Kammeyer and Luiten, 2015; Kendall and Feghali-Bostwick, 2014; Pittayapruek et al., 2016).

Currently, therapy treatment for premature aging still uses topical medications containing retinoic acid, niacinamide, hyaluronic acid, vitamin C, and hydroquinone compounds. It uses even more aggressive therapies such as chemical peels, microdermabrasion, botox injections, and filler injections to laser therapy, which is not fully suitable for all skin types. Therefore, searching for phytoextract compounds to prevent and treat premature skin aging remains necessary (Rosi Helfrich et al., 2008; World Health Organization, 2015). *Molineria latifolia* (Dryand. ex W.T. Aiton) Herb. Ex Kurz *(*family *Hipoxidaceae*) is a plant distributed in Tana Toraja Regency (3°06'42.4"S 119°50'56.3" E), South Sulawesi, Indonesia. In general, *M. latifolia* plants were found in many countries and have been reported to have pharmacological effects (Mad Nasir et al., 2021).

Traditionally, the root of *M. latifolia* was used as a sun-protective powder by the Toraja people in South Sulawesi, Indonesia. Empirically, the community has observed that using this powder from *M. latifolia* root has made the skin less wrinkled and brighter. Research by Nur et al. (2022) has shown that the extract of *M. latifolia* can protect the skin from UV-A and UV-B radiation *in vitro*, but the protection against UV radiation might not be the only reason for producing the less wrinkled and brighter effects. But in the molecular mechanism, intrinsic factor in the form of UV light is one of the factors that can mediate the occurrence of the premature skin aging process. Exposure to UV rays can modulate the increased production of MMPs by ROS and MAPK pathways, leading to skin wrinkles and skin sagging (Amaro-Ortiz et al., 2014; Panich et al., 2016). It is, therefore, interesting to check whether *M. latifolia* extract can inhibit the skin degrading enzyme that causes aging, such as collagenase, gelatinase, and hyaluronidase. If proven, this extract will be a very good candidate to be developed as a skin care product or as a source of active compounds that can be isolated and later developed as synthetic ingredients for skin treatment agents.

Therefore, the phytocomponents of *M. latifolia* as anti-aging through a molecular docking approach to MMPs target proteins, including collagenase (MMP-1) and gelatinase (MMP-9), and hyaluronidase, were evaluated. The resulting specific binding interactions provide an overview of the inhibition of the target protein so that it can be used as a reference for further research as a dermal antiaging agent.

MATERIAL AND METHODS

Ligand preparation

The ligands represented in this study are secondary metabolites of *M. latifolia* obtained from previously reported studies (Mad Nasir et al., 2021; Umar et al., 2021; Wang et al., 2021; Zabidi et al., 2019; 2021). The identified ligands from *M. latifolia* and native ligands were traced through the chemical structure of the PubChem database (https://pubchem.ncbi.nlm.nih.gov/). The ligands used in this study were 46 *M. latifolia* compounds and 3 reference compounds, including retinol (R1), niacinamide (R2), and hyaluronic acid (R3). Data on 46 *M. latifolia* compounds and reference compounds, along with ID codes in the PubChem database, can be seen

in Table 1. All ligands were created in 2D structures using the ChemDraw Ultra 8.0 program in the ChemOffice v.8.0 program package, followed by a 3D structure of the ligand built using Chem3D v.8.0 in the ChemOffice v.8.0 (*mol) program package (www.cambridgesoft.com). The 3D structure was then optimized for geometry using the HyperChem Release v8.07 program. The optimized ligand structure was then analyzed for its molecular properties, saved in file format (*.hin), then converted into a file format (*.pdb) with the ArgusLab program package (www.arguslab.com) for further use in the AutoDock Tools v.4.2 program package (Nursamsiar et al., 2020; 2022).

Receptor preparation

The target proteins used in this study were collagenase (MMP-13) with PDB ID: 2D1N, gelatinase (MMP-9) with PDB ID: 1GKC, and hyaluronidase with PDB ID: 1FCV. The three target proteins were obtained from the Protein Data Bank (https://www.rcsb.org/) and visualized in the Discover Studio Visualizer v17.2.0 program package (Nursamsiar et al., 2022; Riwu et al., 2022).

Calculation of physicochemical value based on the Lipinski rule

The physicochemical values were calculated based on the Lipinski rule consisting of molecular weight, log P, hydrogen bond donors, and acceptors using the HyperChem Professional® v.8.00 and Marvin® v.21.16 (www.chemaxon.com) program packages (Lipinski, 2004).

Parameters of absorption and distribution

The absorption and distribution parameters were calculated using the Pre-ADMET® program accessed via the https://preadmet.qsarhub.com/ website. The *M. latifolia* and references compound ligands were uploaded as *mol. The program calculated the predicted value of the 24 selected parameters, namely the parameters of Human Intestinal Absorption (HIA), Human colon adenocarcinoma (Caco-2) cells, Mandin Darby Canine Kidney (MDCK) cells, and Plasma Protein Binding (PPB) (Bhhatarai et al., 2016; Han et al., 2019).

Toxicity prediction parameters

Toxicity prediction using the Toxtree® program package by uploading *M. latifolia* and references compounds (ligands) in the file (*mol). Toxicity prediction used the Benigni/Bossa rule-base method to determine carcinogenicity (genotoxic and nongenotoxic) and mutagenic properties (Han et al., 2019).

Docking validation method

Validation was carried out to prove that the selected docking parameters can dock the androgen receptor ligands. Validation was performed using natural ligand redocking into the receptor's active site or protein target (Maghfiroh et al., 2021).

Docking simulation assay

Using the Autodock program, a grid box of MMP-13, MMP-9, and hyaluronidase were formed with dimensions 24 × 40 × 48, 40 × 40 × 40, and 28 × 38 × 26 Å, respectively. The grid box coordinates (x, y, z) of each protein target were 44.32 Å, 25.911 Å, -19.703 Å (MMP-13), 40.166 Å, 14.89 Å, 141.719 Å (MMP-9), and -19.267 Å, 27.643 Å and 16.611 Å on the hyaluronidase enzyme. To cover all amino acid residues that play a role in ligand bonds with elastase and hyaluronidase enzymes. The grid was formed at the site of the bound ligand structure. The information about target proteins and ligands and grid dimensions were stored in (*.gpf) format files. he electrostatic potential map, AutoGrid 4.2 grid map, and calculation results will be saved in a (*.glg) format. Then select the docking tools, choose Lamarckian GA, then save it in a (*.dpf) format file. Docking simulation results were stored in (*.dlg) format (Maghfiroh et al., 2021; Nursamsiar et al., 2020). Retinol, niacinamide and hyaluronan were reference compounds for dermal antiaging.

Data analysis

The data obtained were analyzed at each stage, including the validation of the docking method, the predicted value of the Lipinski rule, the prediction of absorption and distribution, the prediction of toxicity, the chemical interaction of the ligand and target protein, and the free energy of each ligand. The ligand interactions of *M. latifolia* were compared to those of native ligands on target proteins.

RESULTS

Visualization of all ligand and proteins target

All native ligands and ligands from *M. latifolia* were visualized through the Software Discovery Studio Visualizer v4.5 program package. The results of the visualization of the ligands can be seen in Figs. 1 and 2.

Table 1. Compounds (ligands) from *M. latifolia* plants and reference compounds.

No	Ligands	Molecule formula	PubChem ID	References
1	Phloridzin	$C_{21}H_{24}O_{10}$	6072	(Zabidi et al., 2019)
2	Pomiferin	$C_{25}H_{24}O_6$	4871	(Zabidi et al., 2019)
3	Scandenin	$C_{26}H_{26}O_6$	54676535	(Zabidi et al., 2019)
4	Mundulone	$C_{26}H_{26}O_6$	4587968	(Zabidi et al., 2019)
5	Dimethylcaffeic acid	$C_{11}H_{12}O_4$	717531	(Zabidi et al., 2019)
6	Protocatechuic acid	$C_7H_6O_4$	72	(Ooi et al., 2016)
7	Syringic acid	$C_9H_{10}O_5$	10742	(Ooi et al., 2016)
8	Cinnamic acid	$C_9H_8O_2$	444539	(Ooi et al., 2016)
9	Ferulic acid	$C_{10}H_{10}O_4$	445858	(Ooi et al., 2016)
10	Orcinoside H	$C_{27}H_{36}O_{14}$	101494941	(Wang et al., 2021)
11	Orcinol glucoside	$C_{13}H_{18}O_7$	70700401	(Umar et al., 2021)
12	Orcinol glucoside B	$C_{15}H_{21}O_8$	-	(Umar et al., 2021)
13	Curculigoside A	$C_{22}H_{26}O_{11}$	158845	(Wang et al., 2021)
14	Curculigoside B	$C_{21}H_{24}O_{11}$	132567	(Umar et al., 2021)
15	Curculigoside C	$C_{22}H_{26}O_{12}$	102004677	(Wang et al., 2021)
16	Curculigoside D	$C_{22}H_{26}O_{11}$	21580518	(Wang et al., 2021)
17	Curculigenin A	$C_{30}H_{50}O_4$	101618893	(Umar et al., 2021)
18	Curculigosaponin A	$C_{36}H_{60}O_9$	101618894	(Umar et al., 2021)
19	Curculigosaponin D	$C_{42}H_{70}O_{14}$	101618897	(Umar et al., 2021)
20	Curculigosaponin F	$C_{48}H_{80}O_{19}$	101618899	(Umar et al., 2021)
21	Curculigosaponin I	$C_{48}H_{80}O_{18}$	-	(Umar et al., 2021)
22	4-0-caffeoylquinic acid-1	$C_{16}H_{18}O_9$	58427569	This study*
23	5,2,6-Trihydroxy-7,8 dimethoxyflavone-2-0-β-D-glucoside	$C_{23}H_{22}O_{13}$	-	This study*
24	5,7,3,5-Tetrahydroxyflavanone	$C_{21}H_{22}O_{11}$	16215147	This study*
25	1,1,6-Trimethyl-1,2-dihydronaphthalene	$C_{13}H_{16}$	121677	This study*
26	Malvalic acid	$C_{18}H_{32}O_2$	10416	This study*
27	Methyl-3-hydroxy-4-methoxybenzoate	$C_9H_{10}O_4$	4056967	This study*
28	Sugiol	$C_{20}H_{28}O_2$	94162	This study*
29	Aviprin	$C_{16}H_{16}O_6$	17536	This study*
30	Guaiacol	$C_7H_8O_2$	460	This study*
31	Smilaxin	$C_{17}H_{16}O_6$	350961	This study*
32	3-Tert-butyl-4-methoxyphenol	$C_{11}H_{16}O_2$	6932	This study*
33	Stearidonic acid	$C_{18}H_{28}O_2$	5312508	This study*
34	Quercetin	$C_{15}H_{10}O_7$	5280343	This study*
35	Azedarachin C	$C_{32}H_{42}O_{10}$	10348330	This study*
36	Trichosanic acid	$C_{18}H_{30}O_2$	5281126	This study*

Table 1. Compounds (ligands) from *M. latifolia* plants and reference compounds (continued...)

No	Ligands	Molecule formula	PubChem ID	References
37	Lucialdehyde B	$C_{30}H_{44}O_3$	10343868	This study*
38	Monobenzone	$C_{13}H_{12}O_2$	7638	(Zabidi et al., 2019)
39	Hidrokuinon	$C_6H_6O_2$	785	(Zabidi et al., 2021)
40	Frangulin B	$C_{20}H_{18}O_9$	442744	(Zabidi et al., 2021)
41	Ubiquinone	$C_{59}H_{90}O_4$	5354031	(Zabidi et al., 2019)
42	Stigmastan 3,6 dione	$C_{29}H_{48}O_2$	146158184	(Umar et al., 2021)
43	2,3-Dihydroxypropyl oleate	$C_{21}H_{40}O_4$	5283468	(Umar et al., 2021)
44	Hordatine A	$C_{28}H_{38}N_8O_4$	45485025	(Zabidi et al., 2021)
45	Emmotin A	$C_{16}H_{22}O_4$	42608142	(Zabidi et al., 2019)
46	Rubratoksin B	$C_{26}H_{30}O_{11}$	11969548	(Zabidi et al., 2019)
R1	Retinol	$C_{20}H_{30}O$	445354	(Ganceviciene et al., 2012)
R2	Niacinamide	$C_6H_6N_2O$	936	(Ganceviciene et al., 2012)
R3	Hyaluronic acid	$C_{28}H_{44}N_2O_{23}$	24759	(Bravo et al., 2022)

Note: (-) is unknown in PubChem ID. (*) Data not yet published. (R1, R2, R3) are references standard as antiaging drugs.

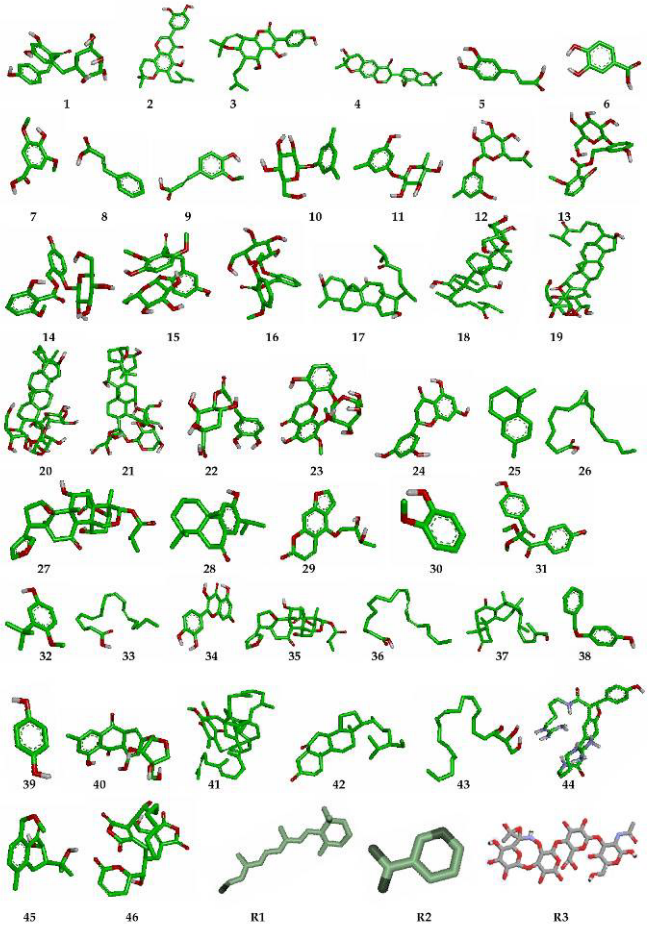


Figure 1. Visualization results of native ligands and *M. latifolia* ligands using the Discover Studio Visualizer v17.2.0 program package.

The names of the ligands were adjusted in the order listed in Table 1. (R1, R2, R3) are references standard as antiaging drugs.

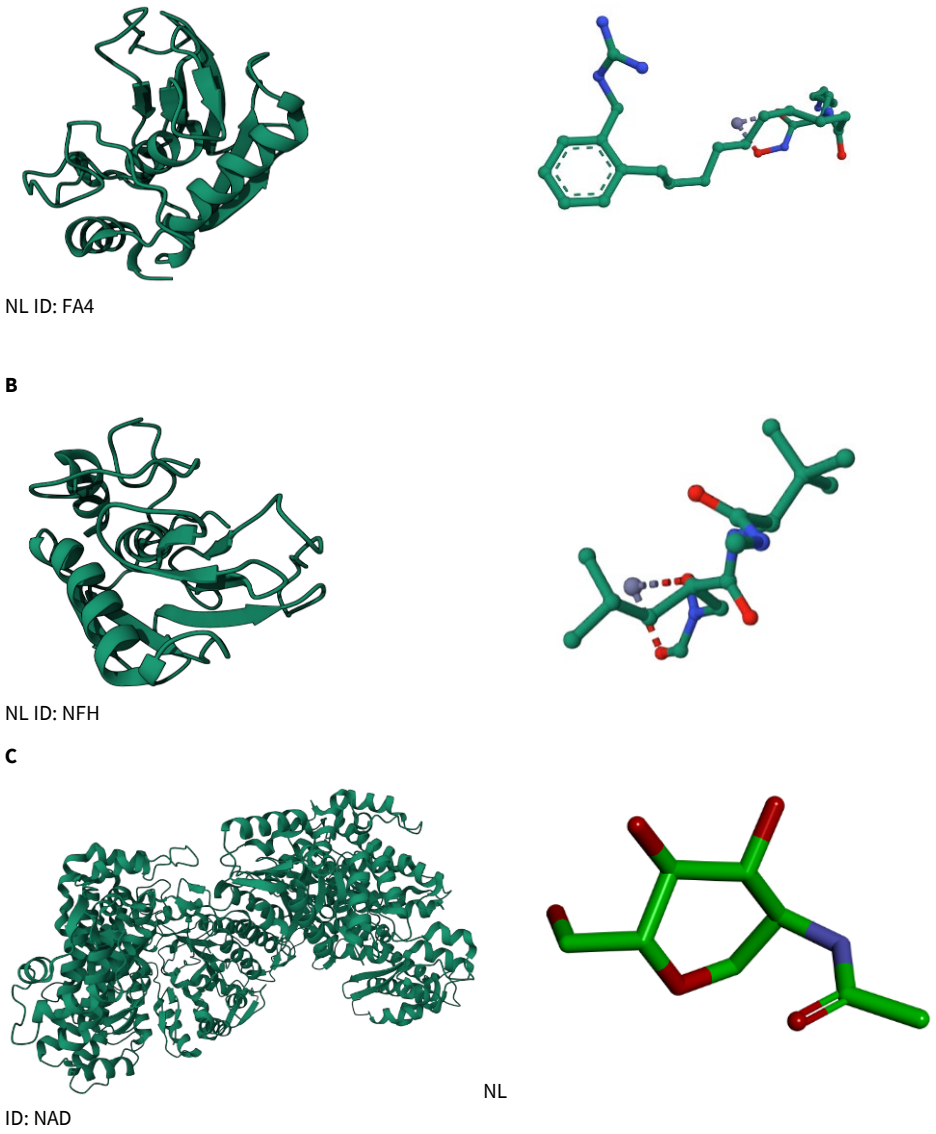


Figure 2. Visualization of target proteins **(A)** MMP-13 (2D1N) with native ligand FA4; **(B)** MMP-9 (1GKC) with native ligand NFH; and **(C)** hyaluronidase (5D1Y) with native ligand NAD.

NL (Native ligand), FA4 (hidroxamic acid, SM 25453), NFH (N~2~-[(2R)-2-{[formyl(hydroxy)amino]methyl}-4-methylpentanoyl]-N,3-dimethyl-L-valinamide), and NAD (2-acetamido-2-deoxy-beta-D-glucopyranose).

Physicochemical value calculation

The calculation of the physicochemical value was determined based on the Lipinski rule. The results of the calculation of the "Five of Rule" physicochemical values *in silico* on ligands from *M. latifolia* indicated that ligands 19, 20, 21, 41, 44, and 46 did not meet the requirements of the Lipinski rule. This is because the six ligands have more than 2 Lipinski rule parameters that exceed the required parameter limits (Table 2). Other ligands (40 ligands) that comply with the Lipinski rule can be considered for development as antiaging agents both orally and topically. Meanwhile, the Lipinski rule analysis of reference compounds tested *in silico* showed that retinol (R1) and niacinamide (R2) complied with the Lipinski rule. However, for hyaluronic acid (R3) compounds, the results unfulfilled.

Absorption and distribution parameter

The *in silico* prediction of ligand absorption from *M. latifolia* was examined based on the ability of the ligand to be absorbed in the gut (human intestinal absorption) and the permeability of the ligand in Caco-2 and MDCK cells. The results of the absorbance prediction study (Table 3) using HIA parameters show that most of the compounds have good absorbance (70-100%). Nonetheless, several compounds, including 1, 12, 14, 19, 22, 23, 34, 40, and 46, can be

Table 2. The results of interpretation of the physicochemical properties of compounds based on Lipinski rules.

Ligands	Lipinski rule					Drug-likeness prediction
	Log P	MW	H-bond donor	H-acceptor	Molar rotation	
Compound 1	0.872	432.00	7*	8	110.93	Comply
Compound 2	5.31*	422.00	3	6	116.97	Comply
Compound 3	5.092*	436.00	2	6	120.43	Comply
Compound 4	4.569	434.00	1	6	120.53	Comply
Compound 5	1.195	180.00	3	4	46.44	Comply
Compound 6	0.796	154.00	3	4	36.73*	Comply
Compound 7	1.107	198.00	2	5	48.17	Comply
Compound 8	1.784	148.00	1	2	43.11	Comply
Compound 9	1.498	194.00	2	4	51.32	Comply
Compound 10	0.517	284.00	4	6	70.31	Comply
Compound 11	0.093	270.00	4	6	65.82	Comply
Compound 12	0.133	312.00	4	7	75.45	Comply
Compound 13	0.054	466.00	5	11*	111.16	Comply
Compound 14	0.357	452.00	6	11*	106.28	Comply
Compound 15	0.349	482.00	6	12*	112.83	Comply
Compound 16	0.239	450.00	4	10	109.50	Comply
Compound 17	5.369*	474.00	3	4	133.91*	Comply
Compound 18	4.496	604.00*	5	7	163.77*	Comply
Compound 19	1.291	782.00*	9	13*	197.79*	Uncompiled
Compound 20	0.884	944.00*	12*	18*	230.43*	Uncompiled
Compound 21	0.143	928.00*	11*	17*	229.01*	Uncompiled
Compound 22	0.645	354.00	6	9	82.51	Comply
Compound 23	0.158	508.00*	6	13	117.73	Comply
Compound 24	2.215	288.00	4	6	71.85	Comply
Compound 25	3.689	172.00	0	0	57.85	Comply
Compound 26	5.862*	280.00	1	2	84.97	Comply
Compound 27	1.187	182.00	1	4	45.99	Comply
Compound 28	4.953	300.00	1	2	88.68	Comply
Compound 29	1.485	290.00	2	6	74.06	Comply
Compound 30	1.400	124.00	1	2	34.65*	Comply
Compound 31	2.152	316.00	2	6	81.62	Comply
Compound 32	2.698	180.00	1	2	53.35	Comply
Compound 33	5.436	276.00	1	2	86.805	Comply
Compound 34	2.010	302.00	5	7	74.05	Comply
Compound 35	3.131	586.00*	2	10	144.49*	Comply
Compound 36	5.660*	278.00	1	2	86.89	Comply

Table 2. The results of interpretation of the physicochemical properties of compounds based on Lipinski rules (continued...)

Ligands	Lipinski rule					Prediction criteria
	Log P	MW	H-bond donor	H-acceptor	Molar rotation	
Compound 37	7.045*	452.00	0	3	132.65*	Comply
Compound 38	2.971	200.00	1	2	58.88	Comply
Compound 39	1.097	110.00	2	2	29.77	Comply
Compound 40	0.108	404.00	5	9	96.14	Comply
Compound 41	17.853*	862.00*	0	4	274.72*	Uncompiled
Compound 42	7.491*	428.00	0	2	127.63	Comply
Compound 43	4.920	356.00	2	4	103.50	Comply
Compound 44	0.962*	550.00*	11*	12*	155.53*	Uncompiled
Compound 45	1.395	278.00	2	4	74.78	Comply
Compound 46	0.697*	518.00*	3	11*	122.88	Uncompiled
R1	3.89	287.00	1	1	94.67	Comply
R2	2.07	194.00	1	2	54.72	Comply
R3	0.48*	777.00*	14*	23*	157.01*	Uncomply

(*) indicates that the predicted physicochemical value does not meet the Lipinski Rule criteria. (R1, R2, R3) are references standard as antiaging drugs.

Table 3. Prediction of the absorption and distribution parameters as well as the toxicity of the ligand.

Ligands	Absorption			Distribution	Carcinogenic		Mutagenic
	HIA (%)	Caco-2 cell (nm/sec)	MDCK cell (nm/sec)	PPB (%)	Genotoxic	Non-genotoxic	
Compound 1	42.94^{b}	19.34^{b}	3.21^{a}	94.83^{a}	Negative	Negative	Negative
Compound 2	92.11^{a}	14.79^{b}	0.04^{b}	96.07^{a}	Positive	Negative	Negative
Compound 3	94.70^{a}	25.65^{b}	0.10^{b}	88.05^{b}	Negative	Negative	Negative
Compound 4	96.38^{a}	35.19^{b}	0.04^{b}	88.49^{b}	Negative	Negative	Negative
Compound 5	82.30^{a}	21.10^{b}	109.43^{a}	40.29^{b}	Negative	Negative	Negative
Compound 6	74.74^{a}	18.30^{b}	23.69^{a}	27.11^{b}	Negative	Negative	Negative
Compound 7	82.02^{a}	18.83^{b}	29.70^{a}	69.77^{b}	Negative	Negative	Negative
Compound 8	97.84^{a}	21.03^{b}	229.47^{a}	60.85^{b}	Negative	Negative	Negative
Compound 9	90.60^{a}	21.11^{b}	228.55^{a}	50.41^{b}	Negative	Negative	Negative
Compound 10	70.31^{a}	2.46^{c}	70.31^{a}	70.31^{b}	Negative	Negative	Negative
Compound 11	2.79^{c}	2.79^{c}	79.52^{a}	52.04^{b}	Negative	Negative	Negative
Compound 12	62.24^{b}	3.86^{c}	4.47^{a}	43.31^{b}	Negative	Negative	Negative
Compound 13	11.83^{c}	11.83^{b}	11.83^{a}	59.98^{b}	Negative	Negative	Negative
Compound 14	33.34^{b}	11.28^{b}	4.62^{a}	60.20^{b}	Negative	Negative	Negative
Compound 15	9.36^{c}	9.36^{b}	1.20^{a}	1.20^{b}	Negative	Negative	Negative
Compound 16	74.48^{a}	14.77^{b}	0.89^{b}	0.89^{b}	Negative	Negative	Negative
Compound 17	91.47^{a}	21.90^{b}	91.47^{a}	97.73^{a}	Negative	Negative	Negative
Compound 18	83.38^{a}	20.97^{b}	0.04^{b}	93.20^{a}	Negative	Negative	Negative
Compound 19	20.25^{b}	20.33^{b}	0.04^{b}	62.67^{b}	Negative	Negative	Negative

Table 3. Prediction of the absorption and distribution parameters as well as the toxicity of the ligand (continued...)

Ligands	Absorption			Distribution	Carcinogenic		Mutagenic
	HIA (%)	Caco-2 cell (nm/sec)	MDCK cell (nm/sec)	PPB (%)	Genotoxic	Non-genotoxic	
Compound 20	2.26[c]	62.67[b]	0.04[b]	37.86[b]	Negative	Negative	Negative
Compound 21	5.18[c]	75.48[a]	0.04[b]	42.37[b]	Negative	Negative	Negative
Compound 22	20.42[b]	42.37[b]	0.74[b]	43.97[b]	Negative	Negative	Negative
Compound 23	28.92[b]	6.77[b]	0.84[b]	51.47[b]	Negative	Negative	Negative
Compound 24	77.4[a]	0.66[c]	39.90[a]	100.00[a]	Negative	Negative	Negative
Compound 25	100.0[a]	23.46[b]	30.66[a]	100.00[a]	Negative	Negative	Negative
Compound 26	98.43[a]	25.06[b]	72.21[a]	100.00[a]	Negative	Negative	Negative
Compound 27	92.23[a]	21.61[b]	40.26[a]	75.44[b]	Negative	Negative	Negative
Compound 28	95.77[a]	75.44[a]	102.57[a]	96.99[a]	Negative	Negative	Negative
Compound 29	92.92[a]	12.39[b]	25.89[a]	77.01[b]	Positive	Negative	Positive
Compound 30	96.46[a]	29.43[b]	362.86[a]	99.17[a]	Negative	Negative	Negative
Compound 31	92.55[a]	20.16[b]	243.33[a]	77.28[b]	Negative	Negative	Negative
Compound 32	96.63[a]	43.44[b]	96.63[a]	100.00[a]	Negative	Negative	Negative
Compound 33	98.16[a]	27.86[b]	79.37[a]	100.00[a]	Negative	Negative	Negative
Compound 34	63.48[b]	3.41[c]	13.35[a]	93.23[a]	Negative	Negative	Positive
Compound 35	88.89[a]	21.72[b]	88.89[a]	67.92[b]	Positive	Negative	Positive
Compound 36	98.27[a]	67.92[b]	98.27[a]	98.27[a]	Positive	Negative	Negative
Compound 37	97.37[a]	25.86[b]	0.09[b]	0.09[b]	Positive	Negative	Positive
Compound 38	97.28[a]	0.09[c]	23.73[a]	100.00[a]	Negative	Negative	Negative
Compound 39	87.42[a]	16.54[b]	87.42[a]	87.42[a]	Negative	Negative	Negative
Compound 40	52.19[b]	18.17[b]	8.97[a]	43.85[b]	Negative	Negative	Negative
Compound 41	98.27[a]	57.51[b]	68.01[a]	68.01[b]	Positive	Negative	Positive
Compound 42	99.02[a]	84.85[a]	0.14[b]	100.00[a]	Negative	Negative	Negative
Compound 43	92.56[a]	35.50[b]	72.36[a]	100.00[a]	Negative	Negative	Negative
Compound 44	47.52[b]	11.35[b]	5.09[a]	64.46[b]	Negative	Negative	Negative
Compound 45	91.88[a]	21.69[b]	99.21[a]	63.23[b]	Negative	Negative	Negative
Compound 46	47.00[b]	20.72[b]	0.40[b]	87.10[b]	Negative	Negative	Negative
R1	100[a]	29.21[b]	26.22[a]	100[a]	Negative	Negative	Negative
R2	92.94[a]	20.36[b]	5.70[b]	20.2[b]	Negative	Negative	Negative
R3	0[c]	2.54[c]	0.51[b]	3.15[b]	Negative	Negative	Negative

- **Human intestinal** absorbs (%HIA): 70-100% well absorbed (a), 20-70% moderately absorbed (b), 0-20% poorly absorbed (c); ***In vitro* Caco-2 cell permeability (nm/sec):** >70 higher permeability (a), 4- 70 medium permeability (b), <4 low permeability (c); ***In vitro* MDCK cell permeability (nm/sec):** >10x10-6 cm/s high permeability (a), 1-10x10-6 moderate permeability (b)**; Plasma protein binding** (%)**:** >90 strongly bound (a) < 90% weakly bound (b).
- **A Negative** indicates that the ligand has no toxic effect; **A positive** indicates that the ligand has a toxic effect. The names of the ligands are adjusted in the order listed in Table 1.
- (R1, R2, R3) are references standard as antiaging drugs.

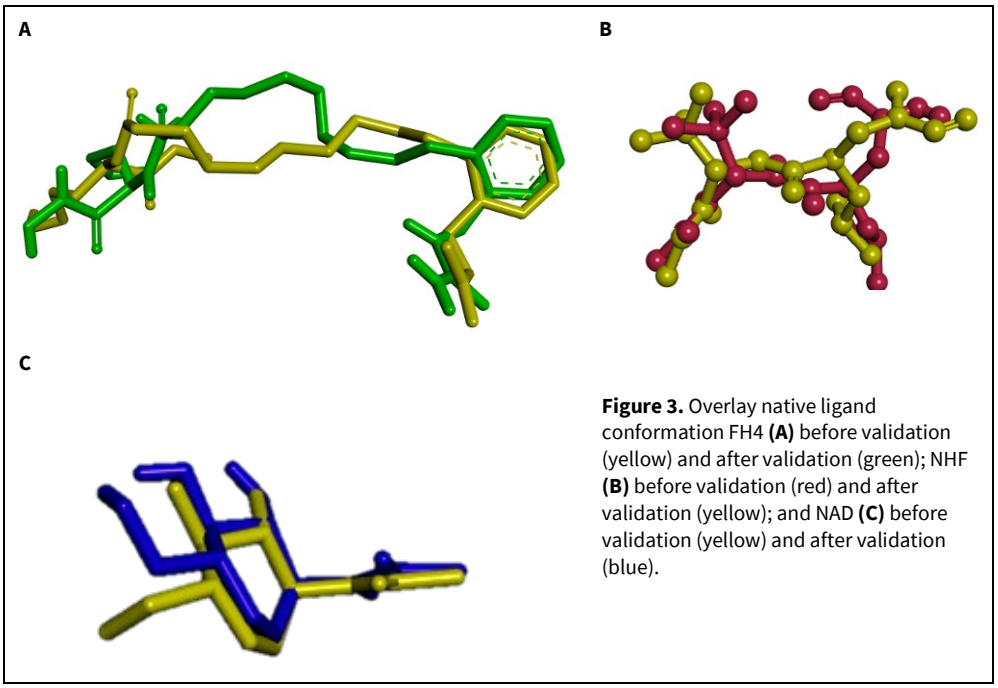


Figure 3. Overlay native ligand conformation FH4 **(A)** before validation (yellow) and after validation (green); NHF **(B)** before validation (red) and after validation (yellow); and NAD **(C)** before validation (yellow) and after validation (blue).

absorbed in the moderate absorption (20-70%) category. In addition, compounds 11, 13, 15, 20, and 21 described a poor absorption profile in the gut with a low category. In permeability analysis, several compounds showed low permeability in Caco-2 cell parameters, namely compounds 10, 11, 12, 24, and 34. Determination of permeability using MDCK cell parameters showed that compounds 2, 3, 4, 16, 18, 19, 20, 21, 22, 23, 37, 42, and 46 have low permeability. While the distribution profile based on plasma protein binding shows that compounds 1, 2, 17, 18, 24, 25, 26, 28, 32, 33, 34, 36, 38, 39, 42, 43, and 46 are highly bound to plasma proteins, therefore it is predicted to have a lower ability of distribution in the body (Table 3). The same thing was found in the reference compounds retinol and niacinamide, which provide pharmacokinetic action in the good absorption phase, but the hyaluronic acid compound provides the opposite (poor absorption). Although the absorption phase shows that the retinol reference compound provides good action, it showed strong binding to plasma proteins in the distribution phase, reducing its distribution in the body. In contrast, the niacinamide compound provided a good distribution action in the body (Table 3).

In silico toxicity prediction

The toxicity prediction study (Table 3) was analyzed using Toxtree software on a Benigni/Bossa rule basis. The results indicated several mutagenic compounds, including 29, 34, 35, 37, and 41. The carcinogenic properties indicated that compounds 29, 35, 36, 37, and 41 were genotoxic carcinogens. Compounds with a genotoxic class cannot be used as additives/drugs because they can cause harmful DNA changes. Non-genotoxic carcinogen analysis showed negative results for all *M. latifolia* ligands. The same results were found for the reference compounds, which showed that the three compounds (R1, R2, and R3) did not have carcinogenic or mutagenic toxic effects.

Docking method validation

Molecular docking method validation was carried out using the AutoDock 4.2 package on target proteins and native ligands. The validation parameter fulfills the validation requirements if the value of RMSD (Root Mean Square Deviation) is less than 2Å. The smaller the RMSD value, the closer the ligand position from the redocking result to the crystallographic result (Kontoyianni et al., 2004). Larger RMSD values cause deviations and errors in predicting interactions between ligands and target proteins (Maghfiroh et al., 2021). Based on the results of the validation analysis of the docking method that has been carried out, the native ligand RMSD values for the target proteins 2D1N (MMP-13), 1GKC (MMP-9), and 1FCV (hyaluronidase) were 1.89; 1.27 and 1.678 Å. The RMSD value obtained for each ligand was <2 Å, so the molecular docking method meets the requirements and has good validity (Nursamsiar et al., 2020). The overlay of the native ligand conformation before and after the validation of the docking method can be seen in Fig. 3.

Docking simulation analysis

Docking simulation of 46 *M. latifolia* ligands and reference compounds against several target proteins, including MMP-13, MMP-9, and hyaluronidase, modulating premature aging formation. Molecular docking aims to predict the ability of the ligand to interact with the target protein, which is assessed based on the bond-free energy and the hydrogen interaction formed. The docking analysis results obtained showed that not all compounds were able to interact well with the target protein. However, several compounds were considered to provide good interactions based on free energy that is more negative and closer to native ligands and patterns of interaction like native ligands key amino acid as positive controls. The bond-free energy value of each ligand to the target protein is presented in Table 4. Molecular interactions between the *M. latifolia* ligand and reference compounds towards the target protein can be seen in Figs. 4, 5, and 6, respectively.

Fig. 4 describes the interactions between the native ligand (FH4) and the *M. latifolia* ligand on the 2D1N target protein. Molecules from native ligands involve various interactions at the key amino acid receptor 2D1N, providing bond-free energy of -10.30. Native ligands interact by hydrogen bonding to the key amino acids Phe241, Ala238, Pro236, Ile243, and Ala186 in the 2D1N target protein. Native ligands also show the presence of van der Waals bonds at Thr247, Phe252, Val219, Leu185, and Leu184. Pi-alkyl interactions with Leu218 and salt bonds with Glu223 also occur in the visualization of these native ligands. The interaction in the native ligand with the key amino acid of the 2D1N target protein is also a parameter that determines the activity of the *M. latifolia* ligand in the inhibiting receptors. Molecular results of the docking of *M. latifolia* ligand against the target protein MMP-13 (2D1N) were interpreted to mean that compounds 17 (curculigenin A), 3 (scandenin), 2 (pomiferin), 4 (mundulone), and 46 (rubratoxin B) have the most negative bond-free energy values, respectively -11.42, -11.25, -10.84, -10.24, and -10.13 kcal/mol. The bond-free energy value of compounds was similar and even more negative than the native ligand (-10.30 kcal/mol). The five compounds also provide an overview of the interactions with the key amino acids of the target protein 2D1N. Compared to the reference compound, it shows similar and even more negative results to the retinol compound (R1) with a binding affinity energy of -10.07 kcal/mol. However, the niacinamide (R2) and hyaluronic acid (R3) compounds provide weak interactions with the 2D1N target protein. This study also showed an interaction between the 2,6-dion stigmastan ligand (compound 42) and MMP-13, which gave a binding affinity of -11.42. The interaction with the key amino acid was not the same as with the native ligand. Therefore this compound was not chosen as the compound that gave the best interaction even though it had a more negative binding affinity value.

Based on the molecular docking of native ligand NHF (N~2~-[(2R)-2-{[formyl(hydroxy) amino] methyl}-4-methylpentanoyl]-N,3-dimethyl-L-valinamide) with protein target 1GKC, 14 linked amino acid residues were obtained including hydrogen bond interaction (Gly186, Leu188, Tyr423, Pro421, Glu402), Van der Waals interaction (Ala189, Leu187, Tyr393, Met422, Tyr420, Glu402), pi-alkyl interaction (Val398, His401), and unfavorable acceptor interaction (His411) with a bond-free energy value of -7.83 kcal/mol (Table 4). Among the compounds docked to the target molecule, 5 compounds have the most negative free energy values and have the profile resemblance of interactions with key amino acids as native ligands. Fig. 5 describes ligand interaction with the target protein MMP-9 (1GKC) showed compounds 4 (mundulone), 3 (scandenin), 46 (rubratoxin B), 1 (phloridzin), and 2 (pomiferin) with bond-free energy values of -9.53, -9.03, -8.67, 8.10 and -7.89 kcal/mol, which is close to the bond free energy value of the native ligand (-7.83 kcal/mol). Whereas the reference compounds in retinol, niacinamide, and hyaluronic acid produced binding free energy to the 1GKC target protein of -8.20, -5.08, and -3.29, respectively. These results indicate that only the retinol references compound has an interaction with bond-free energy similar to the ligand of the *M. latifolia* compound. Meanwhile, niacinamide and hyaluronic acid compounds had lower bond-free energy values than native ligands and ligands from *M. latifolia*.

Whereas in 1FCV, it is interpreted that compounds 25 (1,1,6-trimethyl-1,2-dihydronaphthalene), 12 (orcinol glucoside B), 45 (emmotin A), 11 (orcinol glucoside), and 28 (sugiol) show negative free energy values and were close to the native ligand bond free energy values (-6.39 kcal/mol), namely -6.93, -6.80, -6.73, -6.23, and -5.99 kcal/mol, respectively. The five compounds interact the same way with the native ligands on the 1FCV target protein through hydrogen (light green color) and Van der Waals bonds (faded green color) at the amino acid residues Asn120, Asn223, Tyr168, Phe13, Tyr14, Asp228, Asn257, Gly12, Lys43. In addition, compounds 12, 45, and 28 provide the same pi-sigma (purple color) interaction on the Trp221 amino acid as that of the native ligand. Compounds 11, 12, 25, 28, and 45 showed a better interaction with 1FCV protein than the three reference compounds, namely retinol, niacinamide, and hyaluronic acid (free energy bond, which is more negative than the reference compound). This study also found that

several compounds, including 2, 3, 4, 17-21, 35, 41, and 44, did not bind to the 1FCV target protein, so free energy was not obtained.

Based on the docking simulation results obtained, it was shown that *M. latifolia* compounds in the form of compounds 2 (pomiferin), 3 (scandenin), 4 (mundulone), and 46 (rubratoxin) provide good interactions on the 2D1N and 1GKC target proteins but not on the 1FCV target protein. The compounds orcinol glycosides, orcinol glycoside B, and sugiol, predicted to be active on 1FCV protein, also appear close to the binding affinity values of the native ligands in 2D1N and 1GKC proteins (Fig. 4). Unfortunately, compounds 25 (1,1,6-trimethyl-1,2-dihydro-naphthalene) and 45 (emmotin A) were active on 1FCV but less on 2D1N and 1GKC proteins (Table 4).

Table 4. Molecular docking results of *M. latifolia* ligand against target proteins MMP-13, MMP-9, and hyaluronidase.

Ligand/native ligand	Bond free energy (kcal/mol)		
	2D1N (MMP-13)	**1GKC (MMP-9)**	**1FCV (hyaluronidase)**
NL ID: FH4	**-10.30**	-	-
NL ID: NHF	-	**-7.83**	-
NL ID: NAD	-	-	**-6,39**
Compound 1	-7.34	-8.10	-3.41
Compound 2	**-10.84**	**-7.89**	-
Compound 3	**-11.24**	**-9.03**	-
Compound 4	**-10.24**	**-9.53**	-
Compound 5	-5.04	-5.24	-4.02
Compound 6	-3.81	-4.43	-3.66
Compound 7	-4.20	-4.05	-3.84
Compound 8	-4.80	-4.97	-3.51
Compound 9	-5.13	-5.40	-3.32
Compound 10	-7.34	-7.20	-5.78
Compound 11	-7.81*	-7.71*	**-6.23***
Compound 12	-7.49*	-8.64*	**-6.80***
Compound 13	-6.88	-6.86	-2.59
Compound 14	-6.30	-5.91	-3.79
Compound 15	-6.19	-6.45	-1.56
Compound 16	-7.36	-6.03	-2.80
Compound 17	**-11.42**	-8.62	-
Compound 18	-9.75	-7.78	-
Compound 19	-9.76	-4.88	-
Compound 20	-0.70	-3.06	-
Compound 21	-4.12	-6.15	-
Compound 22	-6.90	-6.24	-3.05
Compound 23	-5.29	-6.23	-2.55
Compound 24	-9.09	-8.65	-5.38
Compound 25	-7.70*	-7.39*	**-6.93**
Compound 26	-5.63	-5.14	-3.42
Compound 27	-6.07	-5.75	-5.03

Table 4. Molecular docking results of *M. latifolia* ligand against target proteins MMP-13, MMP-9, and hyaluronidase (continued...)

Ligand/native ligand	Bond free energy (kcal/mol)		
	2D1N (MMP-13)	**1GKC (MMP-9)**	**1FCV (hyaluronidase)**
Compound 28	-9.12*	-7.79*	-5.99*
Compound 29	-8.34	-7.18	-5.36
Compound 30	-5.04	-4.72	-4.19
Compound 31	-6.57	-7.45	-5.16
Compound 32	-6.14	-6.11	-5.30
Compound 33	-5.99	-5.48	-4.58
Compound 34	-8.51	-7.34	-4.82
Compound 35	-7.85	-5.74	-
Compound 36	-6.74	-5.20	-4.66
Compound 37	-7.98	-7.97	-5.15
Compound 38	-7.44	-7.60	-5.85
Compound 39	-4.92	-4.38	-4.20
Compound 40	-9.55	-8.14	-3.68
Compound 41	-	-1.34	-
Compound 42	-11.21	**-10.98**	-1.05
Compound 43	-7.05	-5.17	-2.43
Compound 44	-9.56	-6.57	-
Compound 45	-6.97	-7.16	**-6.73**
Compound 46	**-10.13**	**-8.67**	-0.91
R1	**-10.72**	-8.20	-5.98
R2	**-5.04**	-5.08	-4.44
R3	**-2.93**	-3.29	-2.88

The bolded letters indicate the ligand that best interacts with the target protein. (-) indicates no interaction between the ligand and the target protein. * Indicates that these compounds can inhibit all three target proteins and interact similarly with native ligands. Samples with codes R1, R2, and R3 were the reference compounds used as comparisons in this study. The names of the ligands are adjusted in the order listed in Table 1.

DISCUSSION

Collagenase (MMP-13), gelatinase (MMP-9), and hyaluronidase are a group of enzymes that mediate the formation of wrinkles on the skin, thereby modulating premature skin aging. Collagenase and gelatinase are matrix metalloproteinases (MMPs) that can degrade molecules such as aggrecan, elastin, fibronectin, gelatine, laminin, and collagen (Nur et al., 2021; Van Doren, 2015). On the other hand, hyaluronidase is an endoglycosidase enzyme that breaks down hyaluronic acid, an extracellular matrix component, into monosaccharides by breaking their glycosidic bonds in connective tissue. When developing drug candidates as antiaging skin drugs, a first approach is needed to minimize failure and search for effective antiaging drugs (Jung, 2020).

In this study, molecular docking analysis was performed on compounds identified in *M. latifolia* plants. *In silico* studies of *M. latifolia* compounds were compared with reference compounds claimed as antiaging compounds, including retinol, niacinamide, and hyaluronic acid, in cosmetic products and have been successfully marketed. Retinol compounds are retinaldehyde derivatives that exhibit antiaging effects caused by extrinsic and intrinsic factors. Retinol can metabolize collagen in tissues so that it has a cell regeneration effect. Niacinamide is also reported to have antiaging effects by increasing collagen metabo-

lism and cell regeneration. Several studies have also reported that niacinamide increases skin elasticity and prevents skin erythema and pigmentation (Ganceviciene et al., 2012; Kafi et al., 2007). The same thing was also reported on hyaluronic acid compounds as antiaging. Hyaluronic acid clinically shows the ability to moisturize the skin and increase its elasticity and prevent wrinkles from occurring (Bravo et al., 2022). These three reference antiaging compounds have generally been applied clinically in topical cosmetic use (Ganceviciene et al., 2012) and use as reference compounds in this research.

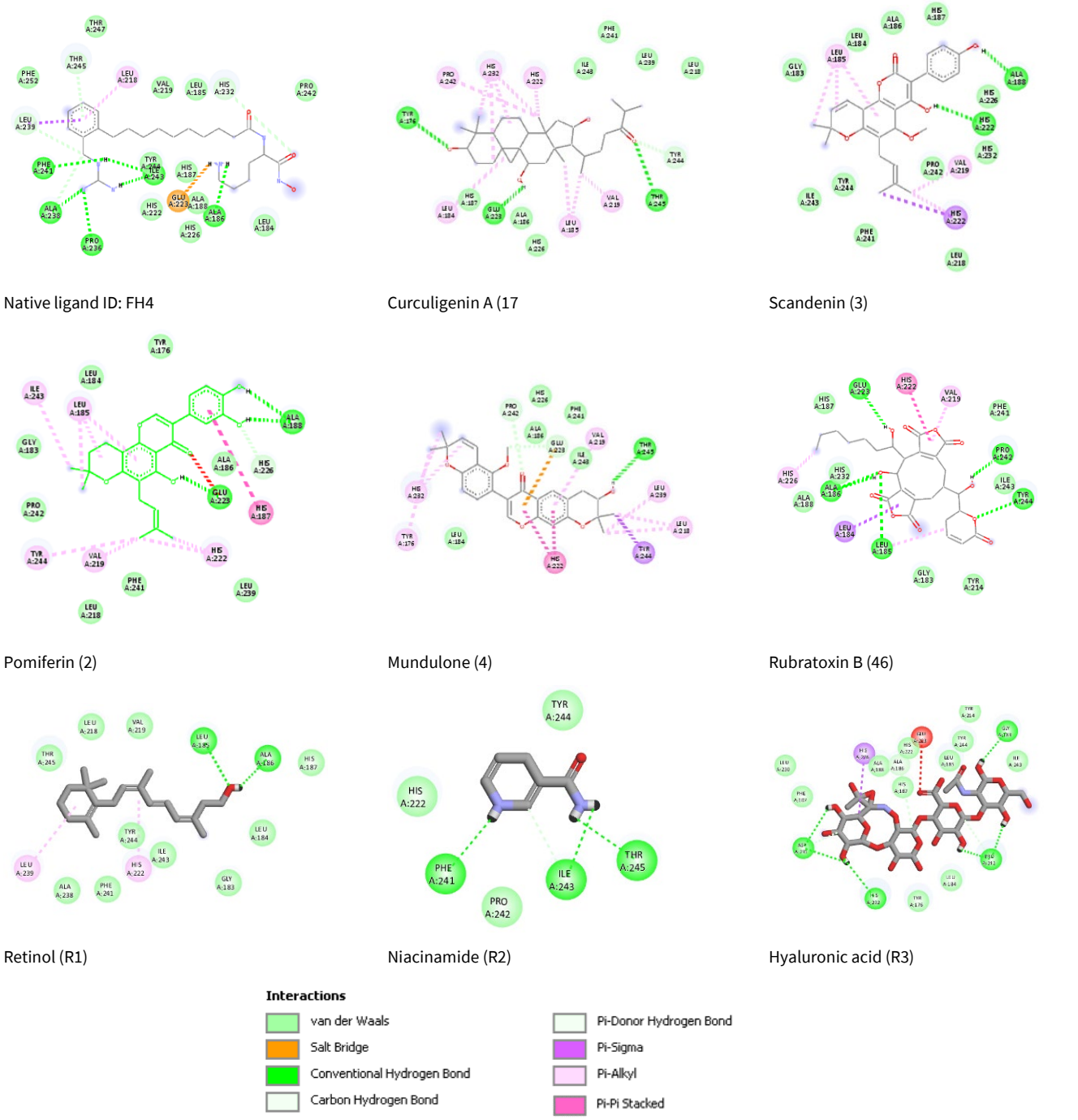


Figure 4. Visualization of the molecular docking results of the ligand from *M. latifolia* and reference compounds and its interactions with the target protein 2D1N (MMP-13).

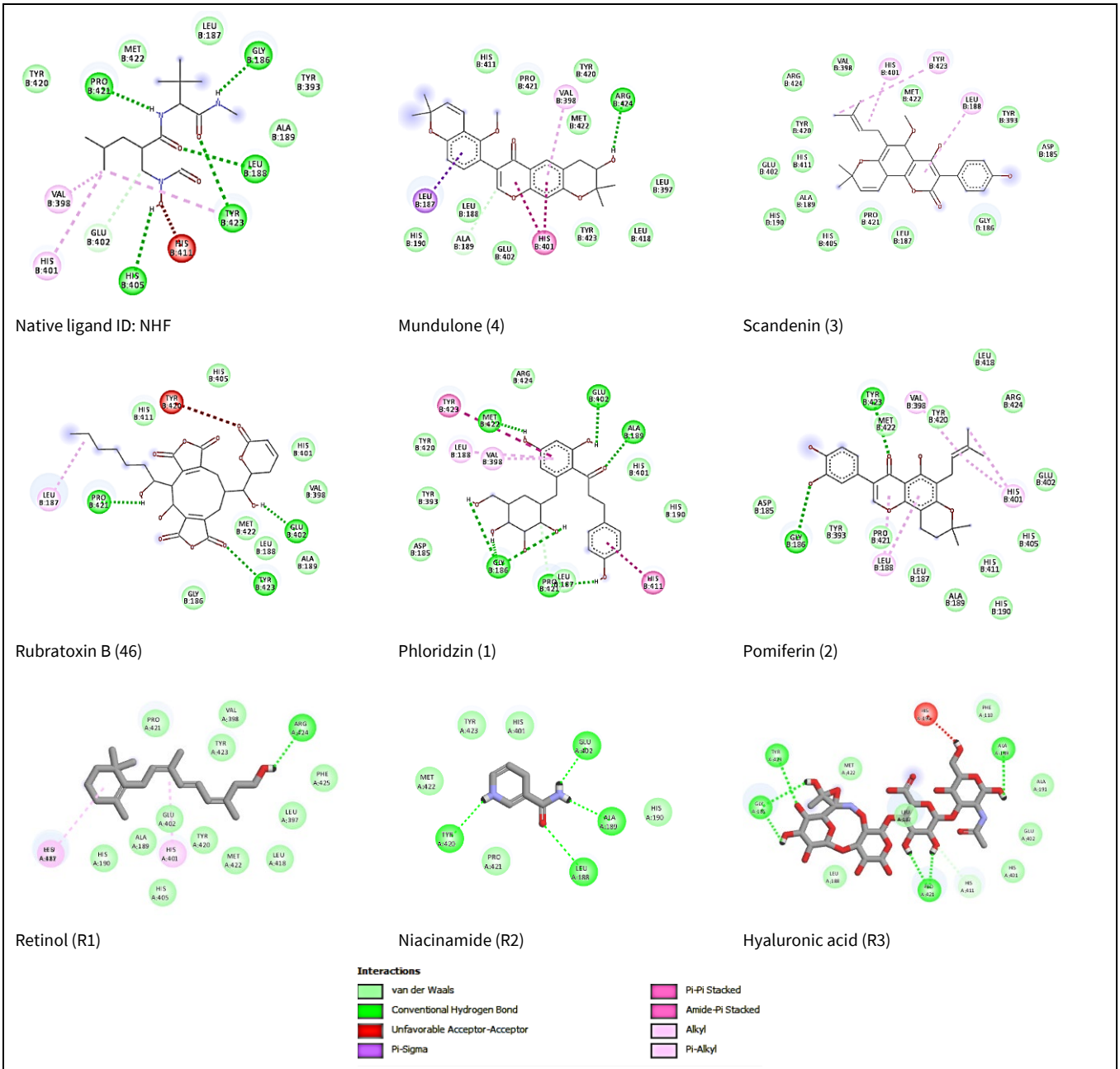


Figure 5. Visualization of the molecular docking results of the ligand from *M. latifolia* and reference compounds and its interactions with the target protein 1GKC (MMP-9).

These studies aim to observe the potential of *M. latifolia* compounds that can interact with skin tissue-degrading proteins that cause premature aging. The compound's ability to inhibit the target protein's action through molecular docking was predicted based on the free energy of binding and the nature of the interaction formed. In addition, solubility and permeability analysis of compounds through biological membranes is important in drug development. Permeability prediction is necessary to prevent drug development failures caused by poor absorption or permeation of drug candidates. An experimental computer model is one approach that can be used to estimate the solubility and permeability of drug candidates (Bennion et al., 2017; Brocke et al., 2019). According to Lipinski's rules, in the development and discovery of drug candidates for oral use, five conditions must be met, known as the rule of five, namely, a drug candidate must have a molecular weight of no more than 500 Dalton, hydrogen bond donors no more than 5, bond acceptors hydrogen is no more than 10, Log P is no more than 5 and molar rotation between 30 to 130 (Lipinski, 2004; Riwu et al., 2022).

Compounds with a molecular weight greater than 500 Daltons have poor permeability or permeation. The log P value suitable for oral use is a value greater than one and less than five to have the ability to cross the bilayer membrane well. Compounds with a log P

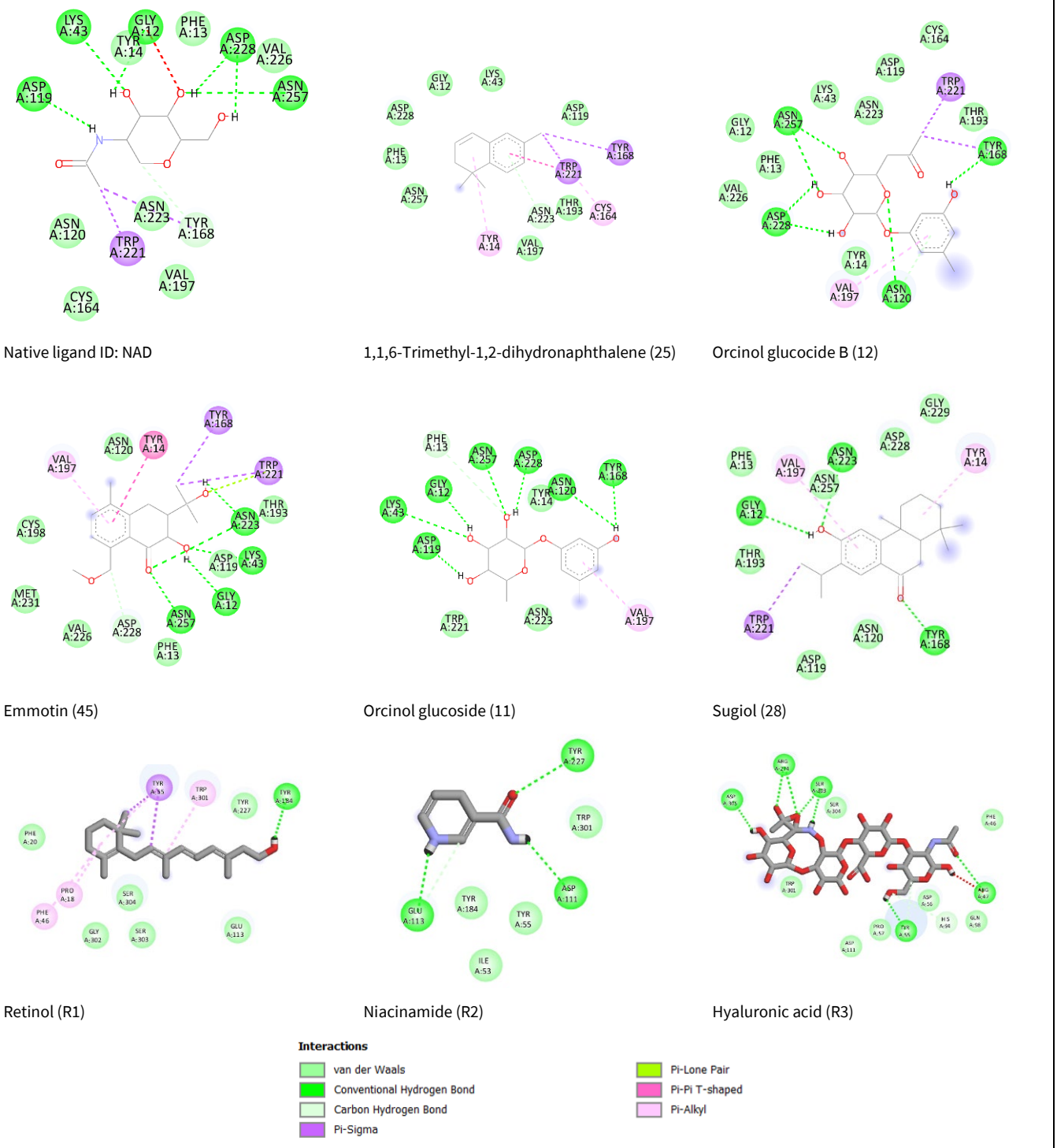


Figure 6. Visualization of the molecular docking results of the ligand from *M. latifolia* and reference compounds and its interactions with the target protein 1FCV (hyaluronidase).

value greater than five may also exhibit toxic properties due to their low solubility in water, making elimination difficult and accumulating in the body (Gao et al., 2017; Riwu et al., 2022). The hydrogen bond donor and acceptor value above the limit also gives a poor permeability profile. It has a large spatial conformation, making it difficult to bind to proteins or receptors. The presence of drug compatibility with a receptor is also influenced by molar rotation. The results in Table 2 show that 40 compounds were deemed eligible to be developed that satisfy at least 3 to 5 parameters of Lipinski's rule (Adianingsih et al., 2022; Riwu et al., 2022). Six compounds were deemed unqualified, including curculigosaponin D, curculi-

gosaponin F, curculigosaponin I, ubiquinone, hordatin A, and rubratoxin B. Almost all these compounds failed Lipinski's rules. This shows that the compound does not have a physicochemical profile consistent with drug-likeness. According to Lipinski et al. (2012), the system recognizes the failure of two parameters or criteria as a warning of poor absorption and permeability. However, these terms do not constitute a restriction or prohibition on drug modifications and further research.

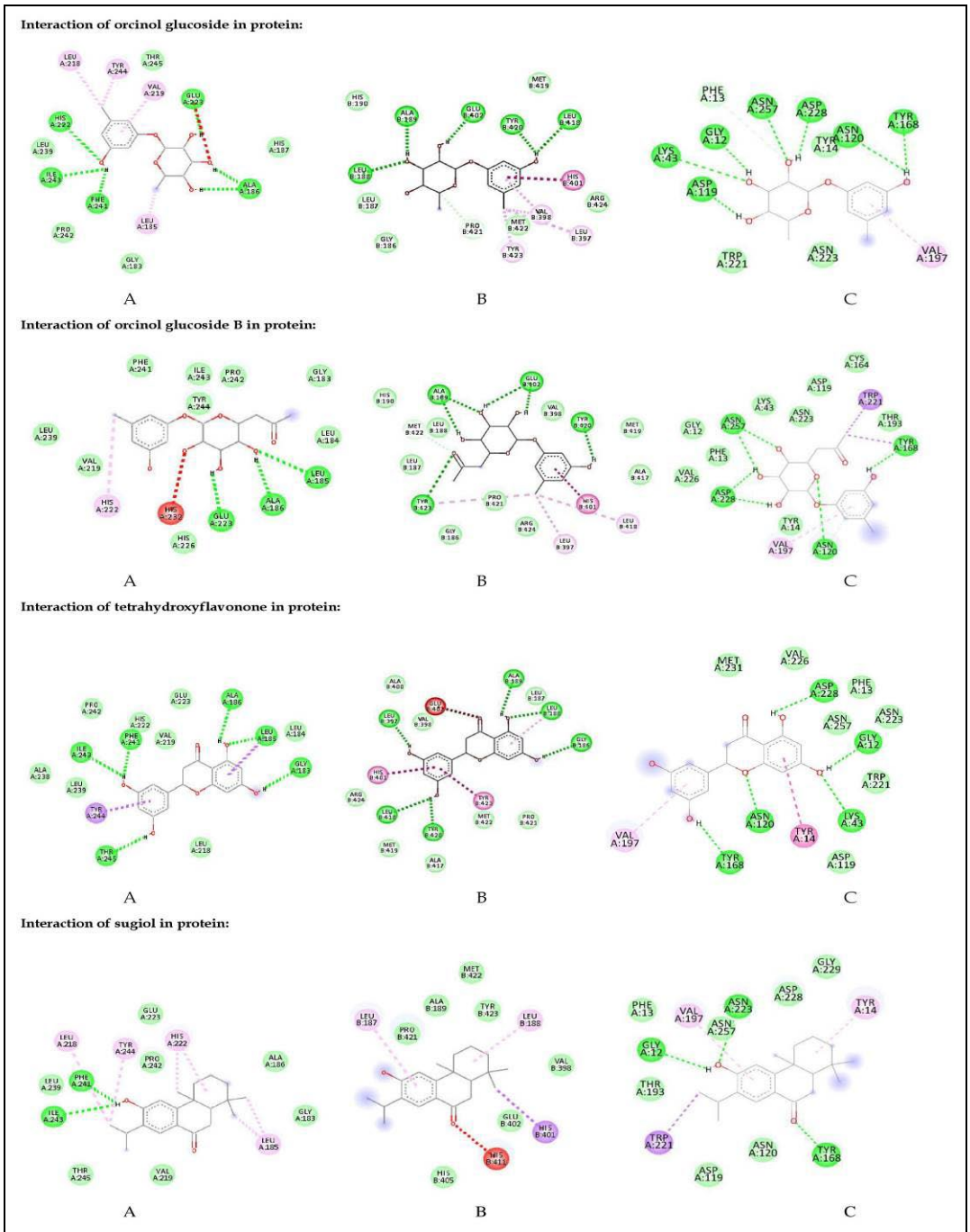


Figure 7. Visualization of the molecular docking results of the ligand and its interactions with the target protein **(A)** 2D1N, **(B)** 1GKC, and **(C)** 1FVC.

The four compounds interact similarly with key amino acids, including Glu223, Ala186, Phe241, Ile243, Leu239, His222, Gly183, Val219, Leu185 and Thr245 in the 2D1N protein. Interaction with Leu187, Gly186, Met422, Arg424, Leu188, Ala189, Glu402, Tyr420, Lei418, Val398, Leu397, and Pro421 in 1GKC. Interaction with Tyr14, Phe13, Asn223, Trp221, Lys43, Asp119, Gly12, Asn257, Asp228, Asn120, Tyr168, Val197 with protein 1FCV. The interactions that occur in each ligand were hydrogen bonds (light green), van der Waals bonds (light green), carbon-hydrogen bonds (dim green), pi-pi-T shaped (light pink), pi-alkyl (pale pink) and pi-sigma (purple).

Retinol (R1) is the most active reference compound for the three target proteins. Retinol interacts with protein amino acid residues 2D1N, 1GKC, and 1FCV, similar to native ligands and active compounds from *M. latifolia*. The interactions of retinol compounds with each target protein can be seen in Figs. 4, 5, and 6.

The ability of a drug molecule to go through a good absorption and distribution phase was also studied in silico. Absorption prediction studied using Human Intestinal Absorption (HIA) is a parameter used to view the percentage of absorption in the human gut. HIA is the sum of bioavailability and absorption assessed by the ratio of urinary, bile, and fecal excretion (Nicolas et al., 2017). Parameters Caco-2 cells are derived from the human colon and undergo multiple cycles of drug transport across the intestinal epithelium. The permeability coefficient is expressed as the permeability of Caco-2 monolayer cell cultures (Volpe, 2011). Caco-2 and MDCK cell models correlate with human intestinal absorption and allow mechanistic assessment of drug permeability, such as passive diffusion (paracellular, transcellular). Thus, the model serves as a rapid screening tool for drug permeability and transport, providing information at the cellular level. These two models are used to predict permeability based on molecular descriptors exploring transporter uptake and efflux mechanisms (DiMarco et al., 2017; Volpe, 2011). While predictions in the distribution phase use Plasma Protein Binding (PPB) parameters. These parameters aim to estimate the level of plasma protein binding based on compounds' molecular and physicochemical properties (Ghafourian and Amin, 2013).

The analysis of the absorption and distribution phases of the 46 *M. latifolia* compounds showed different profiles (Table 3). Several compounds offer absorption and distribution profiles ranging from poor to very good. This is strongly influenced by the physicochemical properties of the connecting molecules, which were also different (Table 2). Nevertheless, the predictions of these compounds still need to be strengthened by various analyses, both *in vitro* and *in vivo*. These studies in pharmacokinetic silico analysis were still limited to the adsorption and distribution phase. In the meantime, the prediction of the metabolic and excretion phases of the 46 compounds of *M. latifolia* needs to be developed for further research.

Toxicity analysis of the compound molecules was also performed in this study. The toxicity prediction of the *M. latifolia* compound using the Benigni/Bossa rule base method analyses the estimated toxicity based on the structure of the compound. Four levels were evaluated in this analysis: Structural Alert for Genotoxic Carcinogenicity, Structural Alert for Non-Genotoxic Carcinogenicity, Negative for Genotoxic Carcinogenicity, and Negative for Non-Genotoxic Carcinogenicity. The drug candidates were expected to have negative carcinogenic genotoxic and carcinogenic non-genotoxic scores (Adianingsih et al., 2022; Benigni et al., 2008). However, based on the analysis results, it was established that compounds 2 and 36 (predicted to be positively genotoxic) and compounds 29, 34, 35, 37, and 41 showed positive genotoxic and mutagenic effects. Meanwhile, non-genotoxic carcinogen was negatively predicted for all compounds of *M. latifolia*. Based on carcinogenicity (genotoxic and non-genotoxic) and mutagenicity rule base of ISS, the test compounds were divided into 10 classes, i.e., Warning structure for genotoxic carcinogens (class 1), warning structure for non-genotoxic carcinogens (class 2), potentially mutagenic Salmonella typhimurium TA100 based on QSAR (Quantitative Structure-Activity Relationship) (class 3) non-potentially mutagenic *Salmonella typhimurium* TA100 based on QSAR (class 4), potentially carcinogenic based on QSAR (class 5) is not potentially carcinogenic based on QSAR (class 5). 6); QSAR calculation can be used for better assessment (class 7), negative for genotoxic carcinogens (class 8), negative for non-genotoxic carcinogens (class 9), and error in the application of the decision tree (class 10) (Benigni et al., 2008; Nohmi, 2018). Therefore, compounds 29, 34, 35, 37, and 41 were categorized as classes 1, 5, and 9, and 2 and 36 as classes 3 and 9. Meanwhile, the other compounds were categorized as classes 8 and 9 (Table 3). The toxicity of these compounds is influenced by the presence of heterocyclic functional groups in their confirmed structures.

Based on the docking results between the compounds and the three receptors, the conformation of the compound with the lowest binding affinity energy was obtained. Binding affinity measures a drug's ability to bind to a receptor. Covalent bonds result in strong affinity and stable and irreversible interactions. Electrostatic bonding can be of strong or weak affinity and is usually reversible. The smaller the binding affinity value, the higher the affinity between the receptor and the compound, and vice versa (Yunta JR et al., 2017; Pantsar and Poso, 2018). The greater the binding affinity value, the lower the receptor and compound affinity. In figures 3, 4, and 5, respectively, interactions that occur between the ligands and the three target proteins show hydrogen bonds such as conventional hydrogen bonds, carbon-hydrogen bonds, and pi-donor bonds; hydrophobic interactions such as pi-alkyl, alkyl, pi-sigma, pi-pi T-shaped, and pi- pi stacked; electrostatic interactions, such as salt bridges, pi-cations, and pi-anions, as well as other interactions.

As a result of the molecular docking approach of the 46 compounds, 5 compounds with the most negative bond-free energy were selected and were close to the native ligands (Table 4). In addition, a similar interaction of the native ligand compounds with the key amino acids of the protein was also observed

(Figs. 3, 4, and 5, respectively). Nonetheless, the predictions of the compounds pomiferin (2), scandenin (3), mundulon (4), and rubratoxin (46) indicate good interaction with both 2D1N and 1GKC target proteins. These four compounds have negative binding affinity values, and some of them have more negative binding affinity than the native ligands FH4 and NHF. But these compounds do not give the 1FCV protein maximum results. These compounds do not show any interaction that occurs with the 1FCV protein. From the *in silico* results, it can be predicted that compounds 2, 3, 4, and 46 could induce inhibition of skin-degrading enzymes in the extracellular matrix tissue, in particular matrix metalloproteinase enzymes (MMP-13 and MMP-9). Although compound 2 (pomiferin) has a negative binding affinity for both 2D1N and 1GKC target proteins, this compound has a positive carcinogenic genotoxic toxicity profile such that the possibility of its use as an oral antiaging candidate is not recommended.

However, upon further analysis, several *M. latifolia* compounds can inhibit the three target proteins with a binding affinity value close to the native ligand (Fig. 7). These compounds include compounds 11 (orcinol glucoside), 12 (orcinol glucoside B), 24 (5,7,3,5-tetrahydroxyflavanone), and 28 (sugiol). The binding affinity energies for the 2D1N target protein were -7.81, -7.49, -7.70, and -9.12 kcal/mol, respectively. In the 1GKC target protein, each compound has a binding affinity value of -7.71, -8.64, -7.39, and -7.79 kcal/mol, respectively. Meanwhile, the target protein 1FCV gave a binding affinity value of -6.23, -6.80, -6.93, and -5.99 kcal/mol, respectively (Table 4). In addition, the results of the drug-likeness analysis predict that compounds 11, 12, 24, and 28 meet the five parameters of Lipinski's rule. The toxicity profile also indicates that the compounds were not expected to have genotoxic and mutagenic effects. Based on HIA parameters, the predicted absorption profile shows that the compound absorbs moderate to high categories. These four compounds were found to have good permeability for the MDCK parameter but low for the Caco2 cell parameter. The distribution profile shows compounds 24 and 28 tightly bound to plasma proteins. Therefore, it is predicted that the distribution process of these compounds in the blood will decrease. However, these deficiencies do not limit the modification of compounds or dosage forms when applied orally.

The reference compound used in this study shows that retinol (R1) provides the best interaction with a bond-free energy value close to that of the native ligand in 2D1N, 1GKC, and 1FCV proteins. Meanwhile, the reference compounds niacinamide and hyaluronic acid provide weak interactions on the three target proteins with a higher bond-free energy value than the native ligands and active compounds from *M. latifolia*. The retinol compound has a similar action to the four compounds from the *M. latifolia* plant, which work in a multitarget manner on receptors related to dermal aging. It can be stated that the compounds orcinol glucoside, orcinol glucoside B, tetrahydroxyflavone, and sugiol from *M. latifolia* can be candidates for further development as antiaging cosmeceutical active ingredients with the same action or even better than retinol as a reference compound.

Results from in silico studies of various *M. latifolia* compounds indicate that some compounds have been predicted to have antiaging potential, particularly in inhibiting the enzymatic upregulation pathway. Some of them, including pomiferin, scandenin, mundulone, rubratoxin, phloridzin, and curculigenin A, have been predicted to inhibit at least one or two target proteins. Several other compounds can be multi-target protein antiaging, including orcinol glucoside, orcinol glucoside B, tetrahydroxyflavone, and sugiol. The ability to inhibit the target protein can be affected by the presence of functional groups in its chemical structure and interactions with the amino acid residues of the target protein (Alberts et al., 2002). Nevertheless, this study needs to be deepened both *in vitro* and *in vivo* to obtain drug molecule candidates from *M. latifolia* as dermal antiaging agents.

CONCLUSION

In silico studies of *M. latifolia* plant compounds generally yield negative binding affinity energy for the target proteins MMP-13, MMP-9, and hyaluronidase. Pomiferin, scandenin, mundulon and rubratoxin compounds specifically inhibit MMP-13 and MMP-9 target proteins while 1,1,6-trimethyl-1,2-dihydronaphthalene, orcinol glucoside, emmotin A, orcinol glucoside and Sugiol compounds specifically inhibit proteins hyaluronidase targets with a more negative energy binding affinity and exhibit similar interactions with native ligands on target proteins. The compounds orcinol glucoside, orcinol glucoside B, 5,7,3,5-tetrahydroxyflavanone and sugiol have been predicted to be able to act on multiple targets against proteins or antiaging receptors. The in-silico study predicts that compounds can be developed for further exploration of their antiaging activity on the skin.

CONFLICT OF INTEREST

The authors declare no conflicts of interest.

ACKNOWLEDGMENTS

This project received funding from the Indonesian Ministry of Education, Culture, Research and Technology

through a Doctoral Dissertation Grant with contract numbers 091/E5/PG.02.00.PT/2022 and 172.PKS/WRIII-DRP/UI/2022. The author would like to thank colleagues (B. Yasir and N.F. Rahman) and student (M.K. Kalelean) who helped complete this project.

REFERENCES

Adianingsih OR, Khasanah U, Anandhy KD, Yurina V (2022) *In silico* ADME-T and molecular docking study of phytoconstituents from *Tithonia diversifolia* (Hemsl.) A. Gray on various targets of diabetic nephropathy. J Pharm Pharmacogn Res 10: 571–594. https://doi.org/10.56499/jppres22.1345.10.4.571

Alberts B, Johnson A, Lewis J, Raff M, Roberts K, Walter P (2002) Analyzing Protein Structure and Function. In: Molecular Biology of the Cell. 4th ed. New York: Garland Science. Available from: https://www.ncbi.nlm.nih.gov/books/NBK26820/

Amaro-Ortiz A, Yan B, D'Orazio JA (2014) Ultraviolet radiation, aging and the skin: Prevention of damage by topical cAMP manipulation. Molecules 19(5): 6202–6219. https://doi.org/10.3390/molecules19056202

Benigni R, Bossa C, Jeliazkova N, Netzeva T, Worth A (2008) The Benigni / Bossa rulebase for mutagenicity and carcinogenicity – a module of Toxtree. JRC Scientific Reports. EUR 23241 EN – 2008. Luxembourg: European Communities, pp. 70.

Bennion BJ, Be NA, McNerney MW, Lao V, Carlson EM, Valdez CA, Malfatti MA, Enright HA, Nguyen TH, Lightstone FC, Carpenter TS (2017) Predicting a drug's membrane permeability: A computational model validated with *in vitro* permeability assay data. J Phys Chem B 121(20): 5228–5237. https://doi.org/10.1021/acs.jpcb.7b02914

Bhhatarai B, Wilson DM, Parks AK, Carney EW, Spencer PJ (2016) Evaluation of TOPKAT, Toxtree, and Derek Nexus *in silico* models for ocular irritation and development of a knowledge-based framework to improve the prediction of severe irritation. Chem Res Toxicol 29(5): 810–822. https://doi.org/10.1021/acs.chemrestox.5b00531

Bravo B, Correia P, Gonçalves Junior JE, Sant'Anna B, Kerob D (2022) Benefits of topical hyaluronic acid for skin quality and signs of skin aging: From literature review to clinical evidence. Dermatol Ther 35(12): e15903. https://doi.org/10.1111/dth.15903

Brocke SA, Degen A, Mackerell AD, Dutagaci B, Feig M (2019) Prediction of membrane permeation of drug molecules by combining an implicit membrane model with machine learning. J Chem Inf Model 59(3): 1147–1162. https://doi.org/10.1021/acs.jcim.8b00648

Colloca G, Di Capua B, Bellieni A, Fusco D, Ciciarello F, Tagliaferri L, Valentini V, Balducci L (2020) Biological and functional biomarkers of aging: Definition, characteristics, and how they can impact everyday cancer treatment. Curr Oncol Rep 22(11): 115. https://doi.org/10.1007/s11912-020-00977-w

DiMarco RL, Hunt DR, Dewi RE, Heilshorn SC (2017) Improvement of paracellular transport in the Caco-2 drug screening model using protein-engineered substrates. Biomaterials 129: 152–162. https://doi.org/10.1016/j.biomaterials.2017.03.023

Ganceviciene R, Liakou AI, Theodoridis A, Makrantonaki E, Zouboulis CC (2012) Skin antiaging strategies. Dermatoendocrinol 4(3): 308–319. https://doi.org/10.4161/derm.22804

Gao Y, Gesenberg C, Zheng W (2017) Oral formulations for preclinical studies: Principle, design, and development considerations. In: Developing Solid Oral Dosage Forms: Pharmaceutical Theory and Practice: Second Edition, pp. 455–495. https://doi.org/10.1016/B978-0-12-802447-8.00017-0

Ghafourian T, Amin Z (2013) QSAR models for the prediction of plasma protein binding. BioImpacts 3(1): 21–27. https://doi.org/10.5681/bi.2013.011

Han Y, Zhang J, Hu CQ, Zhang X, Ma B, Zhang P (2019) *In silico* ADME and toxicity prediction of ceftazidime and its impurities. Front Pharmacol 10: 434. https://doi.org/10.3389/fphar.2019.00434

Jung H (2020) Hyaluronidase: An overview of its properties, applications, and side effects. Arch Plast Surg 47(4): 297–300. https://doi.org/10.5999/aps.2020.00752

Kafi R, Kwak HSR, Schumacher WE, Cho S, Hanft VN, Hamilton TA, King AL, Neal JD, Varani J, Fisher GJ, Voorhees JJ, Kang S (2007) Improvement of naturally aged skin with vitamin A (retinol). Arch Dermatol 143(5): 606–612. https://doi.org/10.1001/archderm.143.5.606

Kammeyer A, Luiten RM (2015) Oxidation events and skin aging. Ageing Res Rev 21: 16–29. https://doi.org/10.1016/j.arr.2015.01.001

Kendall RT, Feghali-Bostwick CA (2014) Fibroblasts in fibrosis: Novel roles and mediators. Front Pharmacol 5: 123. https://doi.org/10.3389/fphar.2014.00123

Kim M, Park HJ (2016) Molecular Mechanisms of Skin Aging and Rejuvenation. Ch. 4. Shiomi N (ed.). IntechOpen, pp. 57–76. https://doi.org/10.5772/62983

Kontoyianni M, McClellan LM, Sokol GS (2004) Evaluation of docking performance: Comparative data on docking algorithms. J Med Chem 47(3): 558–565. https://doi.org/10.1021/jm0302997

Lipinski CA (2004) Lead- and drug-like compounds: The rule-of-five revolution. Drug Discov Today Technol 1(4): 337–341. https://doi.org/10.1016/j.ddtec.2004.11.007

Lipinski CA, Lombardo F, Dominy BW, Feeney PJ (2012) Experimental and computational approaches to estimate solubility and permeability in drug discovery and development settings. Adv Drug Deliv Rev 64: 4–17. https://doi.org/10.1016/j.addr.2012.09.019

Mad Nasir N, Ezam Shah NS, Zainal NZ, Kassim NK, Faudzi SMM, Hasan H (2021) Combination of molecular networking and LC-MS/MS profiling in investigating the interrelationships between the antioxidant and antimicrobial properties of *Curculigo latifolia*. Plants 10(8): 1488. https://doi.org/10.3390/plants10081488

Maghfiroh K, Widyarti S, Batoro J, Sumitro SB (2021) Ethnopharmacological study of flavonoid compounds in *Magnolia champaca* (L.) Baill. ex Pierre as anti-inflammatory agents by molecular docking. J Pharm Pharmacogn Res 9(5): 584–597. https://doi.org/10.56499/jppres20.1004_9.5.584

Nicolas JM, Bouzom F, Hugues C, Ungell AL (2017) Oral drug absorption in pediatrics: the intestinal wall, its developmental changes and current tools for predictions. Biopharm Drug Dispos 38(3): 209–230. https://doi.org/10.1002/bdd.2052

Nohmi T (2018) Thresholds of genotoxic and non-genotoxic carcinogens. Toxicol Res 34(4): 281–290. https://doi.org/10.5487/TR.2018.34.4.281

Nur S, Angelina AA, Aswad M, Yulianty R, Burhan A, Nursamsiar (2021) *In vitro* antiaging activity of *Muntingia calabura* L. fruit extract and its fractions. J Pharm Pharmacogn Res 9(4): 409–421. https://doi.org/10.56499/jppres20.979_9.4.409

Nur S, Aswad M, Yulianty R, Burhan A, Khairi N, Sami FJ, Nursamsiar (2023) The antioxidant and anti-ageing activity of lyophilisate kersen (*Muntingia calabura* L) fruit *in vitro*. Food Res 7(2): 23–23. https://doi.org/10.26656/fr.2017.7(2).749

Nur S, Setiawan H, Hanafi M, Elya B (2022) *In vitro* ultraviolet (UV) protection of *Curculigo latifolia* extract as a sunscreen candidate. OP Conf Ser: Earth Environ Sci 1116: 012009 https://doi.org/10.1088/1755-1315/1116/1/012009

Nursamsiar, Nur S, Febrina E, Asnawi A, Syafiie S (2022) Synthesis and inhibitory activity of curculigoside A derivatives as potential anti-diabetic agents with β-cell apoptosis. J Mol Struct 1265: 133292. https://doi.org/10.1016/j.molstruc.2022.133292

Nursamsiar, Siregar M, Awaluddin A, Nurnahari N, Nur S, Febrina E, Asnawi A (2020) Molecular docking and molecular dynamic simulation of the aglycone of curculigoside A and its derivatives as alpha glucosidase inhibitors. Rasayan J Chem 13(1): 690–698. https://doi.org/10.31788/RJC.2020.1315577

Ooi DJ, Chan KW, Sarega N, Alitheen NB, Ithnin H, Ismail M (2016) Bioprospecting the curculigoside-cinnamic acid-rich fraction from *Molineria latifolia* rhizome as a potential antioxidant therapeutic agent. Molecules 21(6): 682. https://doi.org/10.3390/molecules21060682

Panich U, Sittithumcharee G, Rathviboon N, Jirawatnotai S (2016) Ultraviolet radiation-induced skin aging: The role of DNA damage and oxidative stress in epidermal stem cell damage mediated skin aging. Stem Cells Int 2016: 7370642. https://doi.org/10.1155/2016/7370642

Pantsar T, Poso A (2018) Binding affinity via docking: Fact and fiction. Molecules 23(8): 1899. https://doi.org/10.3390/molecules23081899

Pittayapruek P, Meephansan J, Prapapan O, Komine M, Ohtsuki M (2016) Role of matrix metalloproteinases in photoaging and photocarcinogenesis. Int J Mol Sci 17(6): 868. https://doi.org/10.3390/ijms17060868

Pyo IS, Yun S, Yoon YE, Choi JW, Lee SJ (2020) Mechanisms of aging and the preventive effects of resveratrol on age-related diseases. Molecules 25(20): 4649. https://doi.org/10.3390/molecules25204649

Riwu AG, Nugraha J, Purwanto DA, Triyono EA (2022) *In silico* analysis of anti-dengue activity of faloak (*Sterculia quadrifida* R. Br) stem bark compounds. J Pharm Pharmacogn Res 10(6): 1006–1014. https://doi.org/10.56499/jppres22.1445_10.6.1006

Rosi Helfrich Y, Sachs DL, Voorhees JJ (2008) Overview of skin aging and photoaging dermatology nursing. Dermatol Nurs 20(3): 177–183.

Umar AH, Ratnadewi D, Rafi M, Sulistyaningsih YC (2021) Untargeted metabolomics analysis using FTIR and UHPLC-Q-ORBITRAP HRMS of two *Curculigo* species and evaluation of their antioxidant and α-glucosidase inhibitory activities. Metabolites 11(1): 42. https://doi.org/10.3390/metabo11010042

Van Doren SR (2015) Matrix metalloproteinase interactions with collagen and elastin. Matrix Biol 44-46: 224–231. https://doi.org/10.1016/j.matbio.2015.01.005

Volpe DA (2011) Drug-permeability and transporter assays in Caco-2 and MDCK cell lines. Future Med Chem 3(16): 2063–2077. https://doi.org/10.4155/fmc.11.149

Wang Y, Li J, Li N (2021) Phytochemistry and pharmacological activity of plants of genus *Curculigo*: An updated review since 2013. Molecules 26(11): 3396: https://doi.org/10.3390/molecules26113396

World Health Organization (2015) WHO. World Report on Ageing and Health 2015.

World Health Organization (2013) World population aging 2013. United Nation, Dep. Econ. Soc. Aff.

Yunta MJR (2017) It is important to compute intramolecular hydrogen bonding in drug design? Am J Model Optim 5(1): 24–57. https://doi.org/10.12691/ajmo-5-1-3

Zabidi NA, Ishak NA, Hamid M, Ashari SE, Mohammad Latif MA (2021) Inhibitory evaluation of *Curculigo latifolia* on α-glucosidase, DPP (IV) and *in vitro* studies in antidiabetic with molecular docking relevance to type 2 diabetes mellitus. J Enzyme Inhib Med Chem 36(1): 109–121. https://doi.org/10.1080/14756366.2020.1844680

Zabidi NA, Ishak NA, Hamid M, Efliza Ashari S (2019) Subcritical water extraction of antioxidants from *Curculigo latifolia* root. J Chem 2019: 8047191. https://doi.org/10.1155/2019/8047191

AUTHOR CONTRIBUTION:

Contribution	Nur S	Hanafi M	Setiawan H	Nursamsiar	Elya B
Concepts or ideas	x	x	x	x	x
Design	x	x	x	x	x
Definition of intellectual content	x	x	x	x	x
Literature search	x		x		x
Experimental studies	x	x	x	x	x
Data acquisition	x	x			x
Data analysis	x		x	x	
Statistical analysis	x		x		x
Manuscript preparation	x		x		
Manuscript editing	x		x	x	
Manuscript review	x	x	x	x	x

Citation Format: Nur S, Hanafi M, Setiawan H, Nursamsiar, Elya B (2023) *In silico* evaluation of the dermal antiaging activity of *Molineria latifolia* (Dryand. ex W.T. Aiton) Herb. Ex Kurz compounds. J Pharm Pharmacogn Res 11(2): 325–345. https://doi.org/10.56499/jppres23.1606_11.2.325

Publisher's Note: All claims expressed in this article are solely those of the authors and do not necessarily represent those of their affiliated organizations, or those of the publisher, the editors and the reviewers. Any product that may be evaluated in this article, or claim that may be made by its manufacturer, is not guaranteed or endorsed by the publisher.

Open Access: This article is distributed under the terms of the Creative Commons Attribution 4.0 International License (http://creativecommons.org/ licenses/by/4.0/), which permits use, duplication, adaptation, distribution and reproduction in any medium or format, as long as you give appropriate credit to the original author(s) and the source, provide a link to the Creative Commons license and indicate if changes were made.